10th International Conference
"Research and Development in Mechanical Industry"
RaDMI 2010
16 - 19. September 2010, Donji Milanovac, Serbia

LOAD ANALYSIS OF THE ARTICULATING BOOM SECTIONS OF THE MOBILE ELEVATING WORK PLATFORM IN RELATION TO THE OPERATOR BASKET POSITION

Nebojša Zdravković[1], Milomir Gašić[2], Mile Savković[3], Goran Marković[4]
[1] Faculty of Mechanical Engineering, Kraljevo, SERBIA, e-mail: zdravkovic.n@mfkv.kg.ac.rs
[2] e-mail: gasic.m@mfkv.kg.ac.rs, [3] e-mail: savkovic.m@mfkv.kg.ac.rs, [4] e-mail: markovic.g@mfkv.kg.ac.rs

Summary: *The structural analysys of typical mobile elevating work platform articulating boom, moving quasi-statically in the vertical plane, has been carried out. Along with certain approximations, a model for calculating the load transmission from basket to the support on the vehicle chassis has been developed. Thus, it made possible to track changeable load conditions of every structure element, as well as to track force changes in hydro cylinders, depending on boom joints' angles and geometric parameters of the boom sections. Analytical forms of boom sections load and hydro cylinders forces enable the optimization of the characteristic boom sections dimensions, cross-sections parameters and hydro cylinders abutment points position. In addition, obtained functions can be used for hydro cylinders and hydro pumps workflow control.*

Keywords: *mobile elevating work platform, articulating boom, load transmission, geometric parameters.*

1. INTRODUCTION

Hydraulic elevating platform is a hoisting device that provides temporary access of men and equipment to hardly reachable spots, which are placed at certain heights (from a few meters to several tens of meters). Named application features distinct them from hoisting devices with permanent access to working places and put them into special purpose construction hoisters.
In contemporary urban conditions, just because of configuration of terrain which has lot of obstacles such as street lights, traffic signs, advertising panels, trees, electric, phone and other public installations, parked cars and other objects, the advantage in exploitation often goes to hydraulic elevating platforms with articulating booms, which are typical representatives of structures with variable geometry [3].
The most important parameters of an elevating platform are, besides the lifting capacity, maximum platform height and horizontal reach. Appropriate way of showing these parameters are working diagrams or usage diagrams, shown in Figure 1. In them, the space of usage is marked as a constelation of working points that elevating platform can achieve.
The most often in use are the hydraulic elevating platforms mounted on vehicle. Such machine is called Mobile Elevating Work Platform - MEWP, [5].

2. BASIC ASSUMPTIONS AND CALCULATION MODEL

Articulating boom with hinged sections is a complex mechanism, which is exposed to various loads such as load weight, self-weight of structure elements, dynamic loads at accelerating and decelerating and wind. It can be taken that on/off switching of hydraulic actuators is slow (gradual), by which the slow initiating and final movements of boom sections are realized. In this way, the dynamic loads are considerably decreased, that is the loads can be considered as quasi-static. If the wind is taken out of consideration as an exceptional type of load, calculation model of boom sections load is shown in Figure 3.

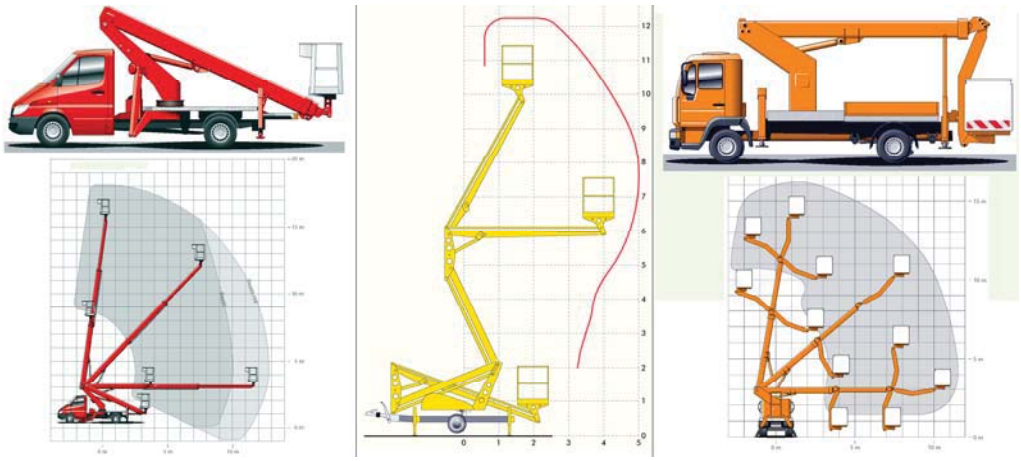

Figure 1: MEWP boom types: telescopic, articulating and combined

Main construction elements of a typical MEWP with articulating boom are shown in Figure 2.

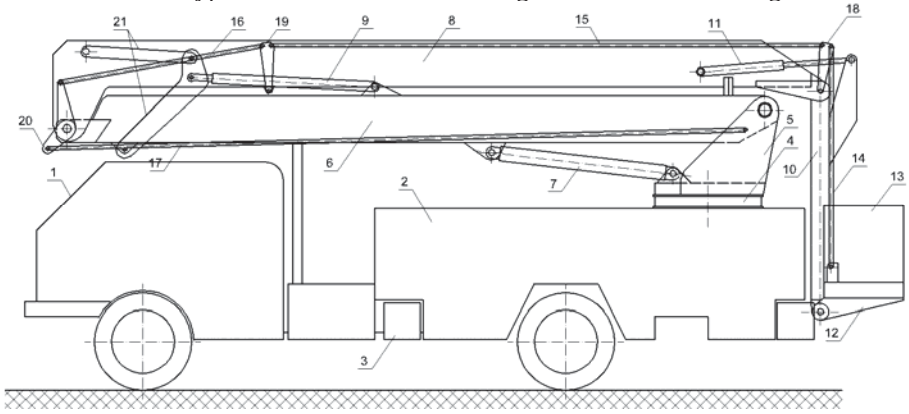

1- Vehicle; 2-Chassis; 3-Outriggers; 4-Revolving bearing; 5-Revolving pillar;
6,8,10-boom sections; 7,9,11-Hydro cylinders; 12-Basket carrier; 13-Basket;
14÷20-Bar system for basket floor horizontality maintenance (leading bars);
21- Bars for boom joint angle increase

Figure 2: Construction elements of a typical MEWP with articulating boom

Sections lengths from one, and appropriate boom joint angles from the other side determine basket position within the work range (lifting height and horizontal reach). The angles defining basket position are those that sections enclose with constant directions: α_1 and α_2 are the angles that sections 1 and 2 enclose with the horizontal direction and α_3 is the angle that section 3 encloses with the vertical direction.

Each section is attached to the local (separate) movable coordinate system ($\xi_i\eta_i\zeta_i$, $i=1,2,3$), at which the coordinate origin is placed at the joint connection with the previous section and ξ_i axes are perpendicular to the figure plane. At the section 1 support, that is the whole boom support, the global coordinate system $AXYZ$ is set. In Figure there is also shown the boom position at maximum joint angles that are: $\alpha_{1max}=75°, \alpha_{2max}=70°, \alpha_{3max}=150°$.

During the work MEWP, there is a number of limitations for angles of sections 1, 2 and 3, which are the result of acting of electrical and mechanical position limiting devices or structure limitations:

$$\alpha_1+\alpha_2 \geq 15°; \alpha_2 \leq \alpha_3 \leq \alpha_2+80°; \alpha_2 < 0° \Rightarrow \alpha_3 = 0°; \alpha_{1max}=75°; \alpha_{2max}=70°; \alpha_{3max}=150°$$

Thus, Table 1 shows the possible combinations of these angles values.

Table 1: Possible combinations of angles α_1, α_2 and α_3 values

$\alpha_1[°]$		75				
		45				
				0		
$\alpha_2[°]$	-60	-30	0	15	45	70
$\alpha_3[°]$	0÷20	0÷50	0÷80	15÷95	45÷125	70÷150

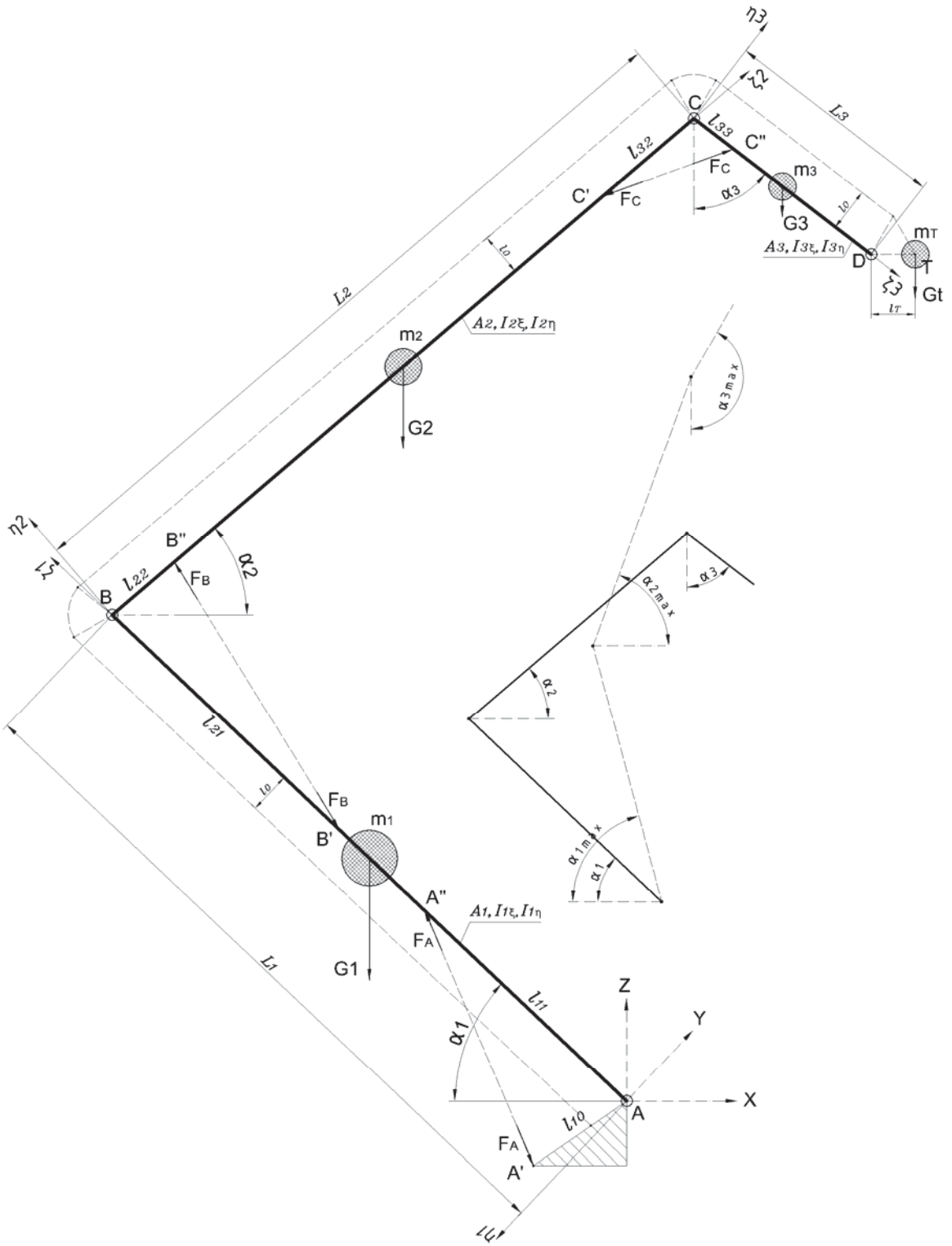

Figure 3: Model for calculation and analysis of boom sections load in relation with basket position

At basket position change, each boom section load is continually changing in the vertical XZ plane. In order to define loads, it is necessary to determine functional relations between all the forces that act on each section and joint angles α_1, α_2 and α_3, as well as forces projections on local coordinate systems. Then, each section can be taken out of the structure and analyzed as separate carrier.

At calculating the forces in relation to the named angles, the sections weights are taken to act in their middle points. Beside this, the model simplifying was done by reducing the influence of forces that act in leading bars on carrying sections, according to figure 4.

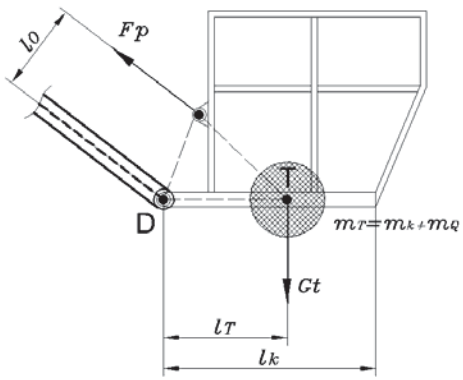

Figure 4: Leading bars forces influence

The leading bars (four bar linkage system) provide the basket floor horizontality and it is taken that they are approximately parallel with boom sections at distance $l_O \approx const$ for any boom position. On this basis, bar extension force is slightly changeable, so it can be, for the sake of simplifying, excluded from analysis. Work load consists of the basket and load mass $m_T = m_k + m_Q$, where m_k stands for basket mass and m_Q stands for mass of the operator and tools in the basket.

3. BOOM SECTION LOAD DETERMINATION IN RELATION TO BASKET POSITION

At determining each boom section load, we must start from section 3, at whose end the reduced weight of basket and load G_T acts. Section 3 calculation model is shown in Figure 5.

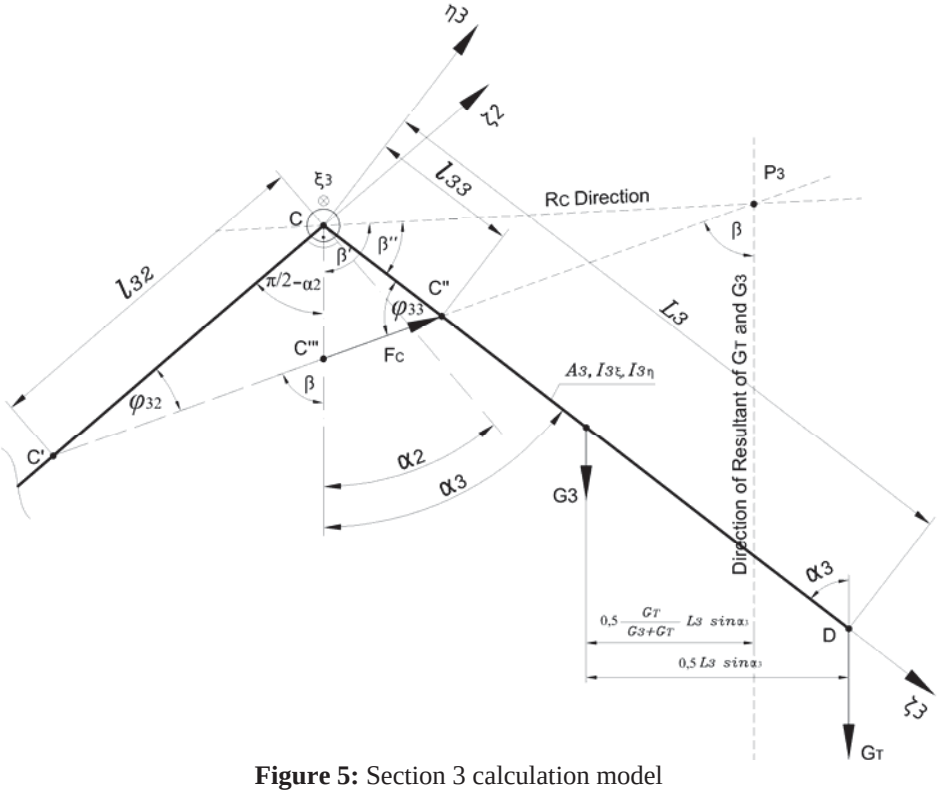

Figure 5: Section 3 calculation model

Force in hydro cylinder F_C is obtained from moment equation for joint C:

$$\sum Mc = 0 \Rightarrow G_T \sin\alpha_3 L_3 + G_3 \sin\alpha_3 \frac{L_3}{2} = F_C \sin\varphi_{33} l_{33} \quad \textbf{(1)}$$

For defining the angle φ_{33}, as well as the other angles which appear in consequent workflow, the sine and cosine theorems are used:

$$\sin\varphi_{33} = \frac{l_{32}}{\sqrt{l_{33}^2 + l_{32}^2 - 2l_{33}l_{32}\sin(\alpha_2 - \alpha_3)}}\cos(\alpha_2 - \alpha_3) \quad \textbf{(2)}$$

It shows that:

$$F_c = \frac{L_3 \sin\alpha_3 \sqrt{l_{33}^2 + l_{32}^2 - 2l_{33}l_{32}\sin(\alpha_2 - \alpha_3)}}{l_{33}l_{32}\cos(\alpha_2 - \alpha_3)}(G_T + 0{,}5G_3) \quad \textbf{(3)}$$

Out of section 3 static equilibrium conditions, we get the reaction of section 2 on section 3 at joint C :

$$R_c = \sqrt{(G_3 + G_T)^2 + F_c^2 - 2(G_3 + G_T)F_c\cos\beta} \quad \textbf{(4)}$$

In order to obtain the diagram of section 3 loads, all the forces should be projected on the local coordinate system $C\xi_3\eta_3\zeta_3$. After adequate angle transformations and equation substitutions, we get the expressions for the force in the hydro cylinder and section 3 loads:

$$F_c = \frac{L_3 \sin\alpha_3 \sqrt{l_{33}^2 + l_{32}^2 - 2l_{33}l_{32}\sin(\alpha_2 - \alpha_3)}}{l_{33}l_{32}\cos(\alpha_2 - \alpha_3)}(G_T + 0{,}5G_3) \quad \textbf{(5)}$$

$$F_{c\eta 3} = F_c \sin\varphi_{33} = \frac{L_3}{l_{33}}(G_T + 0{,}5G_3)\sin\alpha_3 \quad \textbf{(6)}$$

$$F_{c\zeta 3} = F_c \cos\varphi_{33} = \frac{(G_T + 0{,}5G_3)l_3\left[l_{33} - l_{32}\sin(\alpha_2 - \alpha_3)\right]\sin\alpha_3}{l_{33}l_{32}\cos(\alpha_2 - \alpha_3)} \quad \textbf{(7)}$$

$$R_{c\eta 3} = \left[(1 - \frac{L_3}{l_{33}})G_T + (1 - \frac{L_3}{2l_{33}})G_3\right]\sin\alpha_3 \quad \textbf{(8)}$$

$$R_{c\zeta 3} = -(G_T + G_3)\cos\alpha_3 - \frac{(G_T + 0{,}5G_3)l_3\left[l_{33} - l_{32}\sin(\alpha_2 - \alpha_3)\right]\sin\alpha_3}{l_{33}l_{32}\cos(\alpha_2 - \alpha_3)} \quad \textbf{(9)}$$

Section 2 calculation model is shown in Figure 6. Forces F_C and R_C are already defined, but now we take them in opposite directions. Force in hydro cylinder F_B we determine from moment equation for joint B :

$$l_2\cos\alpha_2(G_T + G_3 + 0{,}5G_2) + l_3\sin\alpha_3(G_T + 0{,}5G_3) = F_B\sin\varphi_{22}l_{22} \quad \textbf{(10)}$$

Reaction of section 1 on section 2 in joint B is:

$$R_B = \sqrt{(G_T + G_3 + G_2)^2 + F_B^2 - 2(G_T + G_3 + G_2)F_B\cos\gamma} \quad \textbf{(11)}$$

In order to obtain the diagram of section 2 loads, all the forces should be projected on the local coordinate system $B\xi_2\eta_2\zeta_2$. After adequate angle transformations and equation substitutions, we get the expressions for the force in the hydro cylinder and section 2 loads:

$$R_{c\eta 2} = -(G_3 + G_T)\cos\alpha_2 - \frac{l_3}{l_{32}}\sin\alpha_3(G_T + \frac{G_3}{2}) \quad \textbf{(12)}$$

$$R_{c\zeta 2} = \frac{l_3 \sin\alpha_3(G_T + \frac{G_3}{2})(l_{32} + l_{33}\sin(\alpha_3 - \alpha_2))}{l_{33}l_{32}\cos(\alpha_3 - \alpha_2)} - (G_3 + G_T)\sin\alpha_2 \quad \textbf{(13)}$$

$$F_{c\eta 2} = \frac{l_3}{l_{32}}(G_T + \frac{G_3}{2})\sin\alpha_3 \quad \textbf{(14)}$$

$$F_{c\zeta 2} = -\frac{l_3 \sin\alpha_3(G_T + \frac{G_3}{2})\left[l_{32} + l_{33}\sin(\alpha_3 - \alpha_2)\right]}{l_{33}l_{32}\cos(\alpha_3 - \alpha_2)} \quad \textbf{(15)}$$

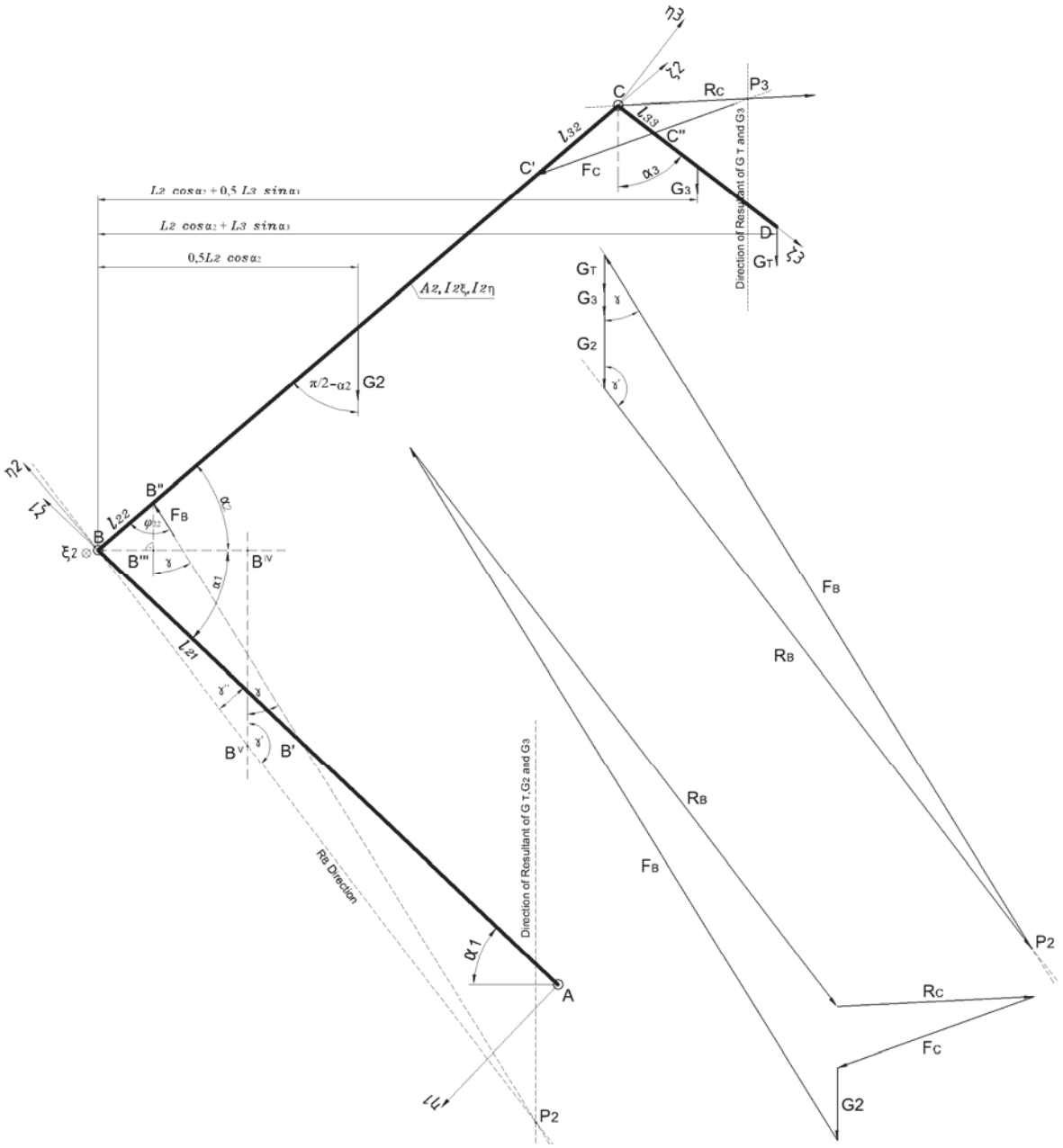

Figure 6: Section 2 calculation model

$$F_B = \frac{\sqrt{l_{21}^2 + l_{22}^2 - 2l_{21}l_{22}\cos(\alpha_1+\alpha_2)}\left[l_2\cos\alpha_2(G_T+G_3+0{,}5G_2)+l_3\sin\alpha_3(G_T+0{,}5G_3)\right]}{l_{21}l_{22}\sin(\alpha_1+\alpha_2)} \tag{16}$$

$$F_{B\eta 2} = \frac{l_2}{l_{22}}(G_T+\frac{G_2}{2}+G_3)\cos\alpha_2+\frac{l_3}{l_{22}}(G_T+\frac{G_3}{2})\sin\alpha_3 \tag{17}$$

$$F_{B\varsigma 2} = \left[l_2\sin\alpha_3(G_T+\frac{G_2}{2}+G_3)\cos\alpha_2+l_3(G_T+\frac{G_3}{2})\sin\alpha_3\right]\frac{l_{22}-l_{21}\cos(\alpha_1+\alpha_2)}{l_{22}l_{21}\sin(\alpha_1+\alpha_2)} \tag{18}$$

$$R_{B\eta 2} = (G_T+G_2+G_3)\cos\alpha_2-\frac{l_2}{l_{22}}\cos\alpha_2(G_T+G_3+\frac{G_2}{2})-\frac{l_3}{l_{22}}\sin\alpha_3(G_T+\frac{G_3}{2}) \tag{19}$$

$$R_{B\varsigma 2} = (G_T+G_2+G_3)\sin\alpha_2 - \frac{\left[l_2\sin\alpha_3(G_T+\frac{G_2}{2}+G_3)\cos\alpha_2+l_3(G_T+\frac{G_3}{2})\sin\alpha_3\right]\left[l_{21}^2+l_{22}^2-2l_{21}l_{22}\cos(\alpha_1+\alpha_2)\right]}{l_{21}l_{22}\sin(\alpha_1+\alpha_2)} \tag{20}$$

Section 1 calculation model is shown in Figure 7. Forces F_B and R_B are already defined, but now we take them in opposite directions. Force in hydro cylinder F_A we determine from moment equation for joint A:

$$l_1 \cos\alpha_1(0{,}5G_1 + G_2 + G_3 + G_T) - l_2 \cos\alpha_2(0{,}5G_2 + G_3 + G_T) - l_3 \sin\alpha_3(0{,}5G_3 + G_T) = F_A l_{11} \sin\varphi_{11} \quad \textbf{(21)}$$

Reaction of boom support in joint A is obtained as follows:

$$R_A = \sqrt{(G_1 + G_2 + G_3 + G_T)^2 + F_A^2 - 2(G_1 + G_2 + G_3 + G_T)F_A \cos\delta} \quad \textbf{(22)}$$

In order to obtain the diagram of section 1 loads, all the forces should be projected on the local coordinate system $A\xi_1\eta_1\zeta_1$. After adequate angle transformations and equation substitutions, we get the expressions for the force in the hydro cylinder and section 1 loads:

$$R_{B\eta 1} = (G_T + G_3 + G_2)\cos\alpha_1 - \frac{l_2}{l_{21}}(G_T + G_3 + \frac{G_2}{2})\cos\alpha_2 - \frac{l_3}{l_{21}}(G_T + \frac{G_3}{2})\sin\alpha_3 \quad \textbf{(23)}$$

$$R_{B\zeta 1} = -(G_T + G_2 + G_3)\sin\alpha_1 + \\ + \frac{\left[l_2 \sin\alpha_2(G_T + \frac{G_2}{2} + G_3)\cos\alpha_2 + l_3(G_T + \frac{G_3}{2})\sin\alpha_3\right]\left[l_{21} - l_{22}\cos(\alpha_1 + \alpha_2)\right]}{l_{21}l_{22}\sin(\alpha_1 + \alpha_2)} \quad \textbf{(24)}$$

$$F_{B\eta 1} = \frac{l_2}{l_{21}}(G_T + \frac{G_2}{2} + G_3)\cos\alpha_2 + \frac{l_3}{l_{21}}(G_T + \frac{G_3}{2})\sin\alpha_3 \quad \textbf{(25)}$$

$$F_{B\zeta 1} = -\left[l_2(G_T + \frac{G_2}{2} + G_3)\cos\alpha_2 + l_3(G_T + \frac{G_3}{2})\sin\alpha_3\right]\frac{l_{21} - l_{22}\cos(\alpha_1 + \alpha_2)}{l_{22}l_{21}\sin(\alpha_1 + \alpha_2)} \quad \textbf{(26)}$$

$$F_A = \frac{l_1 \cos\alpha_1(0{,}5G_1 + G_2 + G_3 + G_T) - l_2 \cos\alpha_2(0{,}5G_2 + G_3 + G_T) - l_3 \sin\alpha_3(0{,}5G_3 + G_T)}{l_{10}l_{11}\sin(\alpha_1 + \alpha_0)} \cdot \\ \cdot\sqrt{l_{10}^2 + l_{11}^2 - 2l_{10}l_{11}\cos(\alpha_1 + \alpha_0)} \quad \textbf{(27)}$$

$$F_{A\eta 1} = -\frac{l_1}{l_{11}}(G_T + \frac{G_1}{2} + G_2 + G_3)\cos\alpha_1 + \frac{l_2}{l_{11}}(G_T + \frac{G_2}{2} + G_3)\cos\alpha_2 + \frac{l_3}{l_{11}}\sin\alpha_3(\frac{G_3}{2} + G_T) \quad \textbf{(28)}$$

$$F_{A\zeta 1} = \left[l_1(G_T + \frac{G_1}{2} + G_2 + G_3)\cos\alpha_1 - l_2(G_T + \frac{G_3}{2})\cos\alpha_2 - l_3 \sin\alpha_3(\frac{G_3}{2} + G_T)\right]\frac{l_{11} - l_{10}\cos(\alpha_1 + \alpha_0)}{l_{11}l_{10}\sin(\alpha_1 + \alpha_0)} \quad \textbf{(29)}$$

$$R_{A\eta 1} = \frac{l_1}{l_{11}}(G_T + \frac{G_1}{2} + G_2 + G_3)\cos\alpha_1 - \frac{l_2}{l_{11}}(G_T + \frac{G_2}{2} + G_3)\cos\alpha_2 - \\ - \frac{l_3}{l_{11}}(G_T + \frac{G_3}{2})\sin\alpha_3 - (G_T + G_1 + G_2 + G_3)\cos\alpha_1 \quad \textbf{(30)}$$

$$R_{A\zeta 1} = (G_1 + G_2 + G_3 + G_T)\sin\alpha_1 - \\ - \left[l_1(G_T + \frac{G_1}{2} + G_2 + G_3)\cos\alpha_1 - l_2(G_T + \frac{G_2}{2} + G_3)\cos\alpha_2 - l_3 \sin\alpha_3(\frac{G_3}{2} + G_T)\right]\frac{l_{11} - l_{10}\cos(\alpha_1 + \alpha_0)}{l_{11}l_{10}\sin(\alpha_1 + \alpha_0)} \quad \textbf{(31)}$$

In Figures 8, 9 and 10 there are shown the diagrams of some of the forces and their projections on local movable axes in relation to α_1, α_2 and α_3 angles. For diagram plotting purpose, the following numerical values were used:

$$L_1 = 7602mm, L_2 = 8210mm, L_3 = 2400mm, l_{33} = 540mm, l_{32} = 1288mm, l_{22} = 876mm, \alpha_0 = 35°,$$
$$l_{21} = 3361mm, l_{11} = 2987mm, l_{10} = 1215mm, G_1 = 15kN, G_2 = 10kN, G_3 = 4kN, G_T = 5kN$$

Negative sign of force value from diagrams tells that the force projection is of the opposite direction in relation to the coordinate axes on which it is projected. Functional relations are shown for some of the section angle values according to Table 1, at which the angles α_1 and α_2 are fixed while the angle α_3 is changing according to structure limitations. While plotting the diagrams, the influence of leading bars force F_P, mentioned in chapter 2, was excluded.

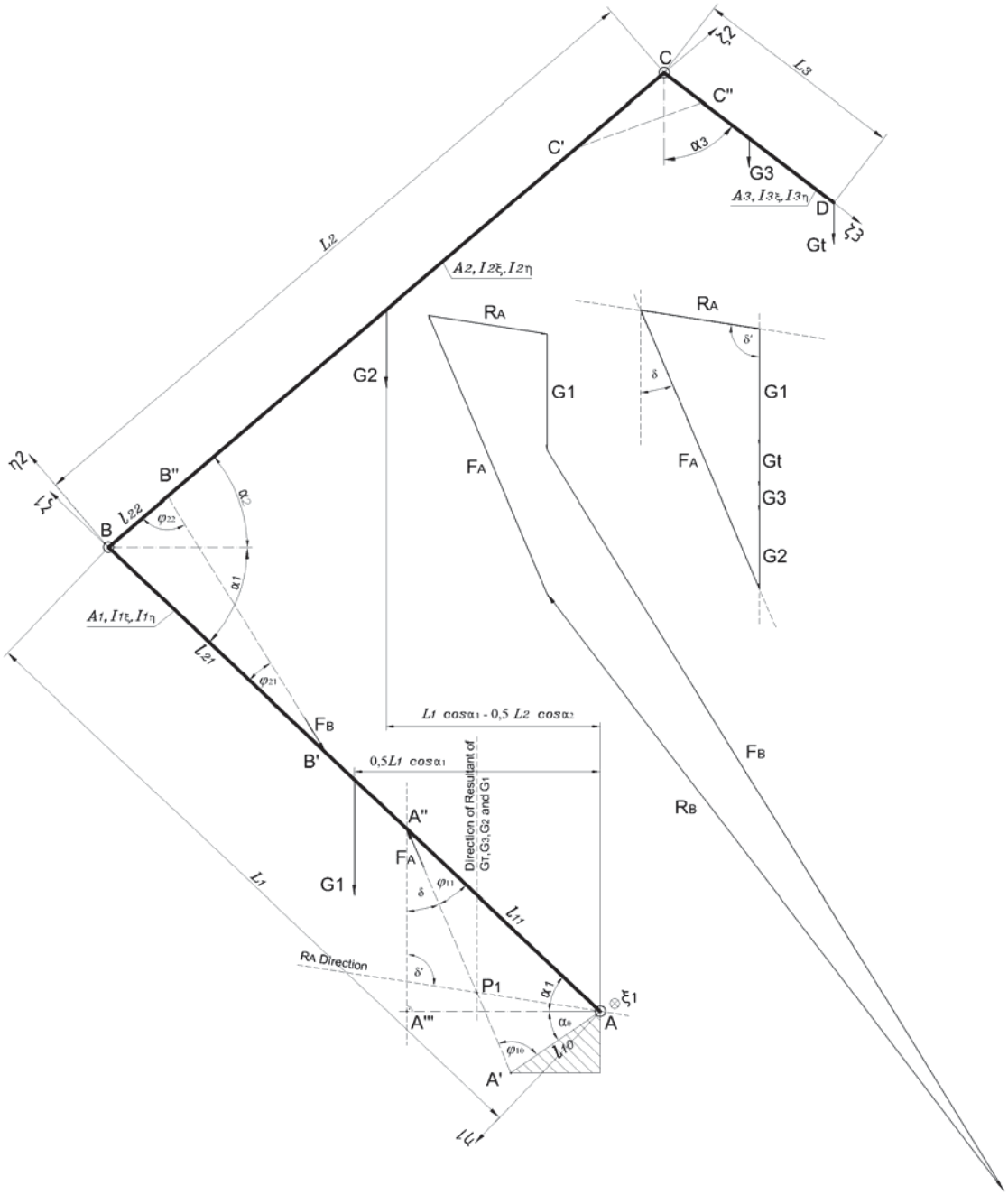

Figure 7: Section 1 calculation model

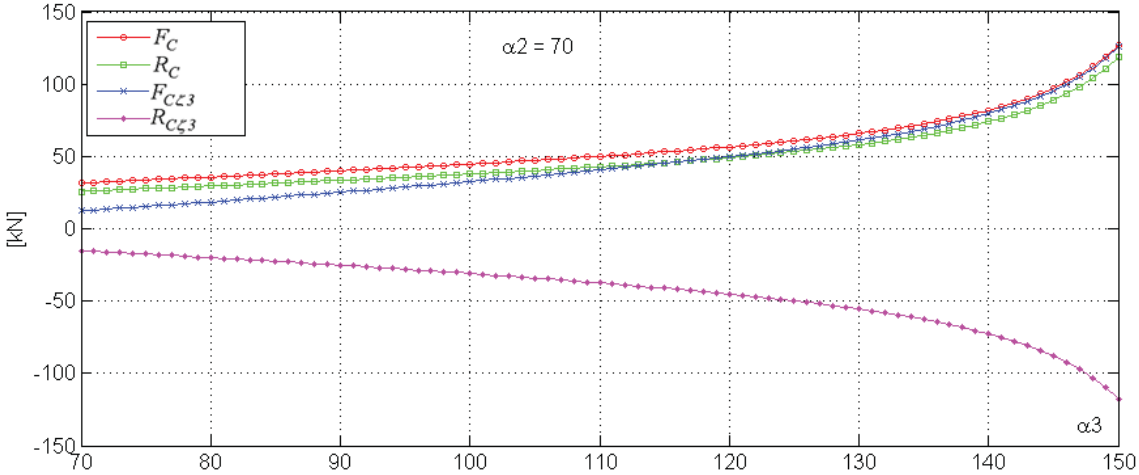

Figure 8: Diagrams F_C , R_C , $F_{C\zeta 3}$ and $R_{C\zeta 3}$ for $\alpha_2 = 70°$ at angle α_3 change

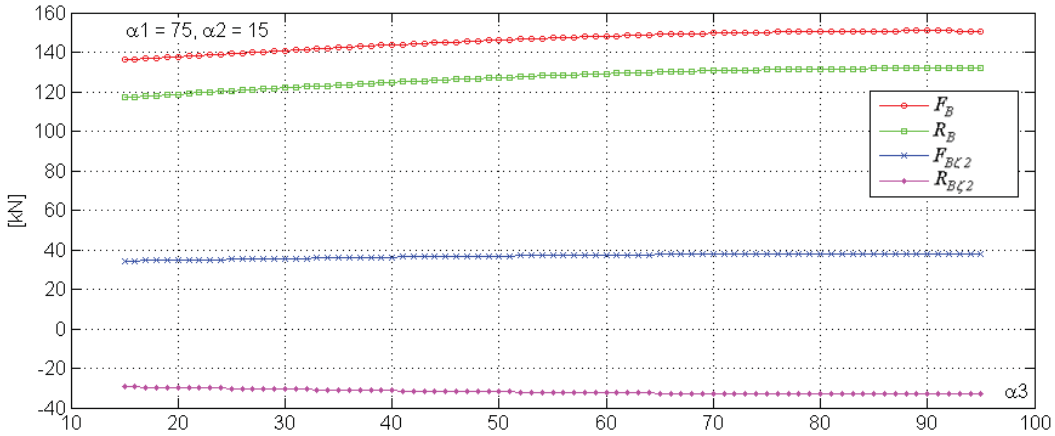

Figure 9: Diagrams $F_B, R_B, F_{B\zeta 2}$ and $R_{B\zeta 2}$ for $\alpha_1 = 75°$ and $\alpha_2 = 15°$ at angle α_3 change

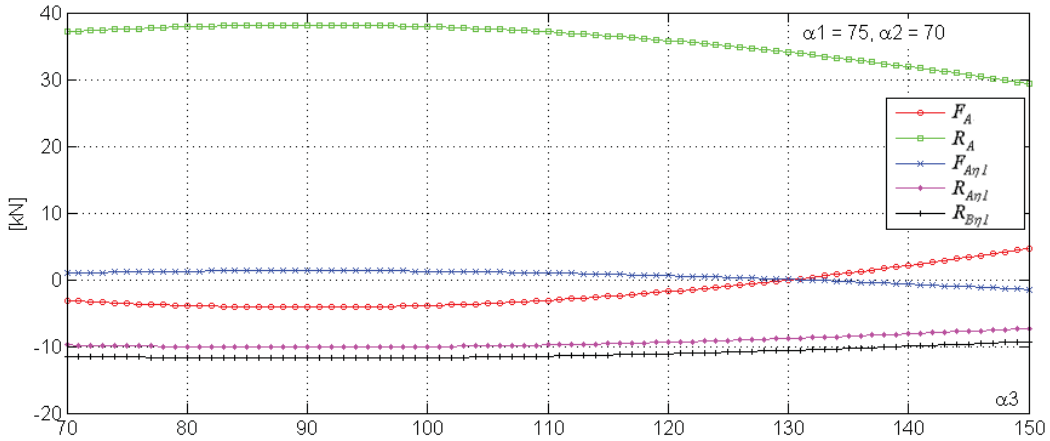

Figure 10: Diagrams $F_A, R_A, F_{A\eta 1}, R_{A\eta 1}$ and $R_{B\eta 1}$ for $\alpha_1 = 75°$, $\alpha_2 = 70°$ at angle α_3 change

4. CONCLUSION

The significance of determining the functional dependences of the MEWP articulating boom sections loads can be seen through the possibility of finding the critical boom positions from the aspect of each structure element. In this way, each element can be analyzed separately with its changeable loads at joints with contiguous elements and hydro cylinders abutments. Analytical forms also open a possibility for software development, which would enable instant generation of all static diagrams for an arbitrary selected basket position within the space of usage.

REFERENCES

[1] Jerman, B.; Kramar, J.: A study of the horizontal inertial forces acting on the suspended load of slewing cranes. *International Journal of Mechanical Sciences*, Volume 50, Issue 3, March 2008, Pages 490-500

[2] Jerman, B.; Podržaj, P.; Kramar, J.: An investigation of slewing-crane dynamics duringslewing motion—development and veri&cation of a mathematical model. *International Journal of Mechanical Sciences*, Volume 46, Issue 5, May 2004, Pages 729-750

[3] Bošnjak, S.; Zrnić, N.; Dragović, B.: Dynamic Response of Mobile Elevating Work Platform under Wind Excitation. *Strojniški vestnik - Journal of Mechanical Engineering*, Vol. 55, No. 2 (2009), pp. 104-113. ISSN 0039-2480.

[4] M. Gašic, M.; Savkovic, M.; Bulatovic, R.; Petrovic, R.: Optimization of a pentagonal cross section of the truckcrane boom using Lagrange's multipliers and differential evolution algorithm. *Meccanica - An International Journal of Theoretical and Applied Mechanics*, DOI 10.1007/s11012-010-9343-7

[5] Radoičić G.: Experimental testing of vibro-confort on mobile elevating work platform, *Research and Design in Commerce & Industry*, No. 11, year IV(2006), pp. 25-35, ISSN 1451-4117.

[6] Farkas Jozsef.: *Optimum Design of Metal Structures*, Akademiai Kiado, Budapest, 1984., ISBN 963-05-3435-5.